Corrosion Fatigue behavior of Submerged Arc Welded high strength steel used in Naval Structures

H. Das and T. K. Pal

Welding Technology Centre, Metallurgical & Material Engineering Department, Jadavpur University, Kolkata-700032, India
d.hrishikesh@yahoo.com; tkpal.ju@gmail.com

ABSTRACT

Corrosion prevention is a major concern for naval structures particularly for welded joint of high strength steel. Although cathodic protection (CP) is still widely used to prevent corrosion of structural steels in marine environment, effectiveness of CP has not been proven for structural steels with a yield stress above 400 MPa. In the present investigation, high strength steel plate of DMR 249A was welded by Submerged Arc Welding (SAW) process and the corrosion fatigue tests were performed on weld metal in air and 3.5% NaCl solution at room temperature with R ratio of 0.1 and a cyclic frequency of 0.01 Hz with and without cathodic potential. Optimum cathodic potential for weld metal was also evaluated in unstressed condition from the minimum corrosion coefficient among four potentials (under at -800, -875, -950, -1025) mV based on potentiostatic polarization curves (E_{corr} value) of weld metal. Corrosion fatigue results suggest that optimum cathodic potential data (-875 mV) determined in unstressed condition could be used to improve the corrosion fatigue life of weld metal used in naval structure.

Key words: High strength steel, SAW, Fatigue Crack Growth Rate (FCGR), Polarization Curve, corrosion coefficient, Corrosion Fatigue.

1.0 INTRODUCTION

Corrosion prevention is a major concern for naval structures. The primary methodology for corrosion control on ship hulls is anti-corrosion epoxy coatings (paints). Anti-corrosion epoxy coatings are typically multi-layer systems that are based on detailed chemical evaluation of the base metal and the proposed operating environment. But no matter how good the paint or coating system, or how well applied, these systems are subjected to mechanical wear and damage, biological attack, improper application and aging with time. The end result is that there will be regions of exposed metal that were originally protected by coatings. In addition, there are multiple inlet and outlet ports for various piping systems as well as other features of the ship on a ship hull. These features and the knowledge that paint damage will occur, has led to the use of secondary systems, such as cathodic protection systems, to provide additional defense against corrosion damage.

Fatigue damage is one of the most important factors to be considered in designing of large welded structures such as ship hull. A ship structure has to withstand loads of different types such as static loads and cyclic loads. For quasi-static wave loads, a conventional life span of 10^8 considered to verify the ship's design, a figure which corresponds approximately to a life span of 20 to 25 years [1]. The number of cycles can differ for other loads (ice impacts, slamming impacts, vibratory responses etc.) and marine environment. Marine structures exposed to severe marine environment should be protected against corrosion in an appropriate way. Cathodic Protection

(CP) is widely used to prevent corrosion of structural steels in marine environment [2]. Most of the accidents occurred recently were associated with the corrosion of welding part and hydrogen embitterment of marine structure steel under cathodic protection [3, 4]. Existing guidance on the design and construction of marine structure does not define the optimum level of CP and notes that the effectiveness of CP has not been proven for structural steels with a yield stress above 400MPa [5]. Thus, there is clearly a need to establish the optimum and safe working limits of CP in realistic environments, if higher strength steels are to be more widely employed in marine structure.

In the present investigation, high strength steel of DMR 249A grade which is currently being used for ship construction in stead of low carbon steel in India, has been welded by Submerged Arc Welding (SAW) process and fatigue crack growth rate (FCGR) has been studied in air and in 3.5% NaCl solution at cyclic frequency of 0.01 Hz with and without CP.

2.0 EXPERIMENTAL PROCEDURE

The low alloy steel plate of DMR 249 A of size 300mm X 150mm X 15mm was used as base metal in this work. Chemical composition and mechanical properties of base metal are given in **Table 1** and **Table 2** respectively.

Steel plates were made double V- Groove of 60° included angle and welded by submerged arc welding (SAW) process. Before welding the plates were surface ground to remove the oxides and dirt. The welding parameters are given in **Table 3**.

The welds were first examined visually followed by X-ray radiography test. The sound welded joints were used to prepare samples for metallography, tensile, charpy impact, fatigue testing (at 0.01Hz) in air and in 3.5% NaCl solution with and without CP.

2.1 Microstructure of base metal and Weldments

The metallography specimens of the weldments were ground and polished using standard method. The polished specimens were etched with 2% nital. The microstructures were studied under optical microscope (Carl Zeiss made: AX10 Imager A1m) and photo micrographs were taken at different magnifications.

2.2 Micro hardness of welded joint

Micro hardness was taken across the weldment using Vickers's hardness testing machine using a load of 100gm.

2.3 Preparation of Samples for FCGR

Single Edge Notch three-point bend sample specimens of 7.2 mm X 15 mm cross section and 80 mm length as per ASTM E647 as shown schematically in **Fig. 1** are used for Fatigue Crack Growth Rate (FCGR) tests in air and in environment. FCGR tests were carried out on a 100 KN servo-electric machine (INSTRON 8862) using software controlled decreasing ÄK envelope with constant R-ratio (0.1) as per ASTM E647. The crack was monitored using a COD gauge with the help of da/dN software.

Table 1: Chemical composition of base metal

Material	C	Si	Mn	S	P	Cu	Ni	Cr	Mo	Nb	Al	Ti	Fe
DMR 249	0.10	0.24	1.6	0.018	0.02	0.312	0.688	0.21	0.02	0.015	0.02	0.016	Bal.

Table 2: Mechanical Properties of base metal

Base Metal	Plate thickness	Y.S (MPa)	UTS (MPa)	% El.
DMR 249A	15 mm	464	607	33

Table 3: Welding Parameters used in SAW process

Welding process	Welding position	Inter pass temp.	Dia. of filler wire	Welding current (A)	Welding voltage (V)	Welding speed cm/min	Heat input kj/mm
SAW	Downhand	150°C	3.2	600	32	30	3.84

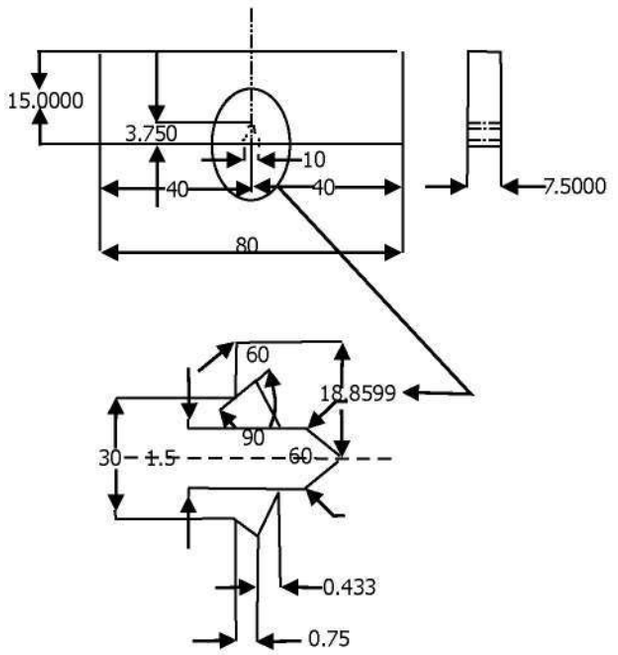

Fig. 1: Schematic diagram of 3 point bend sample

2.4 Potentiostatic Polarization

The potentiostatic polarization curves for base metal, weld metal and HAZ were determined in 3.5% NaCl solution using AUTOLAB PGSTAT 302 Potentiostatic machine at a scan rate of 0.5mv/s using Ag/AgCl electrode as reference and platinum as counter electrode. Tafel's slopes were derived from the polarization curve.

2.5 Cathodic protection without stress

Based on the Ecorr values of base metal, weld metal and HAZ derived from polarization curves, four potentials for each zone (base metal, weld metal and HAZ) were selected to study cathodic protection .The cathodic protection curves for base metal under (at -650, -725, -800, -875) mV, weld metal under (at -800, -875, -950, -1025) mV and HAZ under (at-875, -950, -1025, -1100) mV are evaluated. Corrosion coefficient for each potential in each zone of weldment was evaluated and only minimum corrosion coefficient for base metal, HAZ and weld metal achieved for a given potential are found out. The polarization potential, which attributed minimum corrosion coefficient, were considered as an adequate cathodic protection in corrosion fatigue test.

2.6 Corrosion Fatigue of Weld Metal

For corrosion fatigue tests, a specially fabricated inverted three-point bend fixture shown in **Fig.2a** and schematically shown in **Fig. 2b** along with Teflon sheet chamber of size 360 mm X 266 mm X 150 mm containing about 8 liters of 3.5% NaCl solution were used. The inside of this container was lacquered and the rollers of the bend fixture were Teflon wrapped so that undesirable chemical reaction is prevented. The pH of the bulk solution was monitored at regular intervals and was maintained within 6-7 throughout the test. The corrosion fatigue test was carried out at room temperature with R ratio of 0.1 and a cyclic frequency of 0.01 Hz.

Fatigue Crack Growth Rate (FCGR) tests were carried out on a 100 KN servo-electric machine (INSTRON 8862) using software controlled decreasing ÄK envelope with constant R-

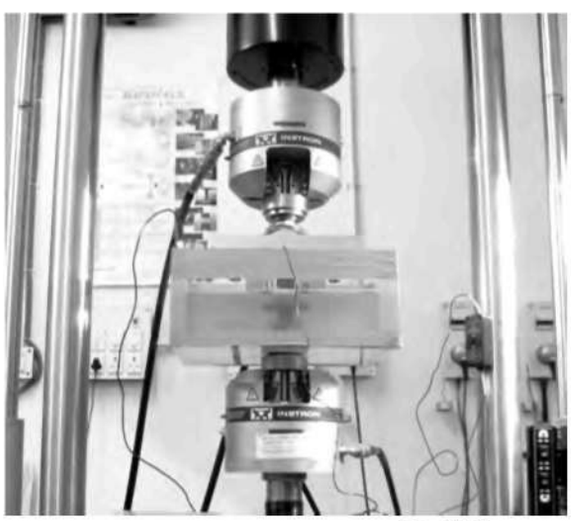

Fig. 2(a)

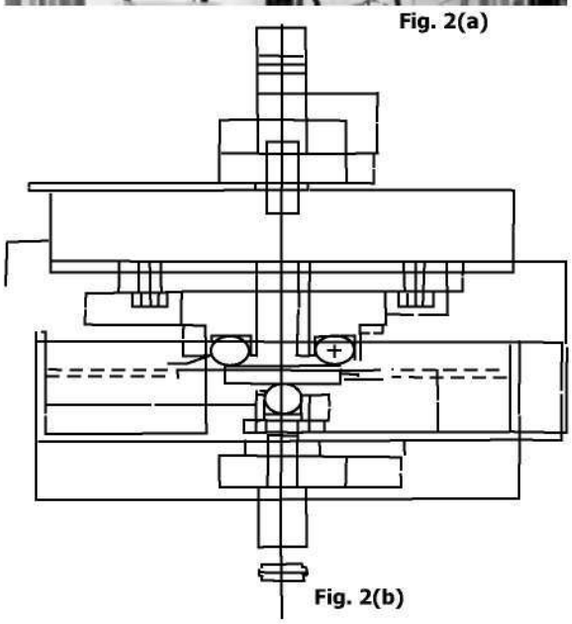

Fig. 2(b)

Fig. 2: (a) Experimental set up and (b) Schematic diagram of 3 point bend fixture fitted with corrosion chamber

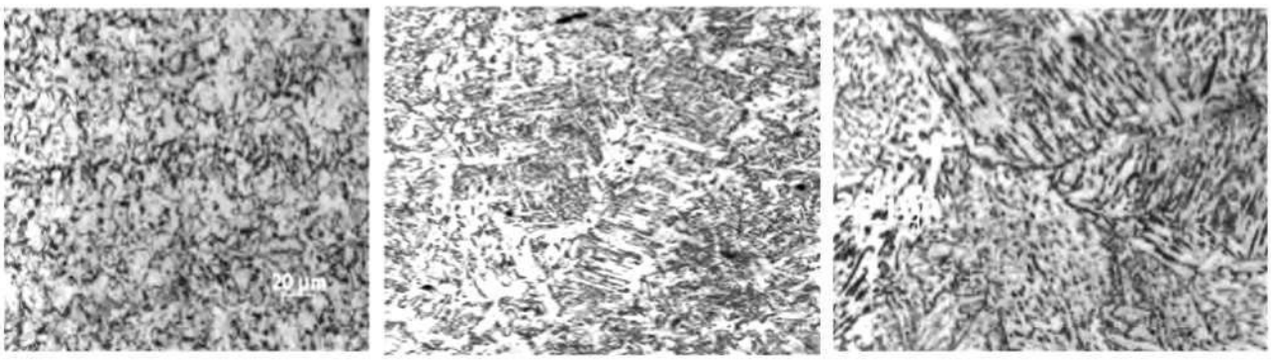

Fig. 3: Microstructure of (a)Base Metal (b) Weld Metal and (c) HAZ in SAW process, X500

ratio (0.1) as per ASTM E647. Crack lengths were measured using a 10 mm gauge length crack opening displacement (COD) gauge fixed on integral knife edges machined samples across the crack mouth.

2.7 Fracture Surface Study

The Fracture surface of welded samples after FCGR tests in air and corrosion medium at R =0.1 and cyclic frequency of 0.01 Hz was observed under SEM.

3.0 RESULTS AND DISCUSSION

3.1 Microstructure of base metal and Weldments

Microstructures of base metal, weld metal and HAZ are shown in **Fig.3.** Microstructure of base metal shows ferrite and pearlite. Pearlite appears as banded structure. On the other hand, weld metal consists of acicular ferrite, grain boundary ferrite, ferrite with aligned second phase along with veins of ferrite. The microstructure of HAZ reveals mostly grain boundary ferrite with aligned second phase within prior austenite grain boundary.

The microstructure depends primarily on the chemical composition and cooling rate. In weld metal, in addition to chemical composition and cooling rate, the presence of inclusion plays an important role in influencing microstructure. On cooling below AC3 temperature, ferrite will start nucleating initially at austenite grain corner and boundaries. Since these sites generally provide lowest energy barrier to nucleation [6], grain boundary ferrite (GBF) occurs over the temperature range 1000 °C to 650 °C [7].

With increasing degree of under cooling, further growth of ferrite can take place by lateral movement of ledges along low energy surface which is characteristics of widmanstatten side plate ferrite structure [6]. Side plate ferrite (SPF) forms between 750 °C and 650 °C [7] and grows from grain boundary ferritic as long needles which protrudes into the austenite grains [6].

Acicular ferrite starts to nucleate intragranulary at inclusions in the transformation temperature range between 630 °C to 450 °C simultaneously with or immediate after the formation of side plate ferrite.

Acicular ferrite are promoted with (i) increased in prior austenite grain size [6], (ii) with increasing element like C, Mn, Mo and possibly Si & Ni [7, 10] by shifting the austenite decomposition transformation to large delay times [8, 9] and (iii) with favorable size, volume fraction and composition of non metallic inclusion [8, 11]. As a result of ferrite formation during cooling in weld metal, carbon is continuously enriched with the remaining austenite depending on cooing rate and weld metal chemical composition. This carbon rich austenite may transform to ferrite with aligned second phase or upper bainite [6] which forms at temperature below 500 °C [7].

The final microstructure in weld metal depends on complex interactions between several important variables such as chemical composition (hardenability element), type, volume fraction, size of inclusions, and cooling rate.

3.2 Micro hardness of welded joint

The micro hardness data across DMR 249 A welded joints are shown in **Fig.4.** Weld metal shows higher hardness than base metal. The hardness of HAZ is in-between.

3.3 Potentiostatic polarization

Potentiostatic polarization study has been done for base metal, weld metal and HAZ shown in **Fig. 5.** From the potentiostatic polarization curves corrosion rate and Ecorr have been evaluated and are given in **Table 4**.

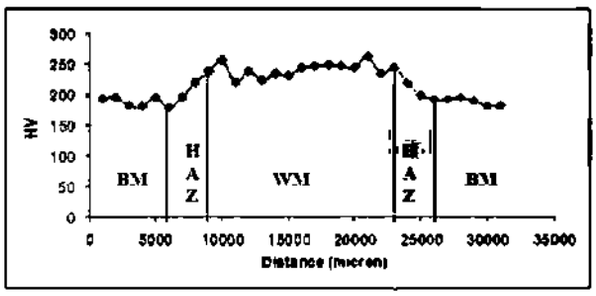

Fig.4: Microhardness of welded DMR 249 A sample

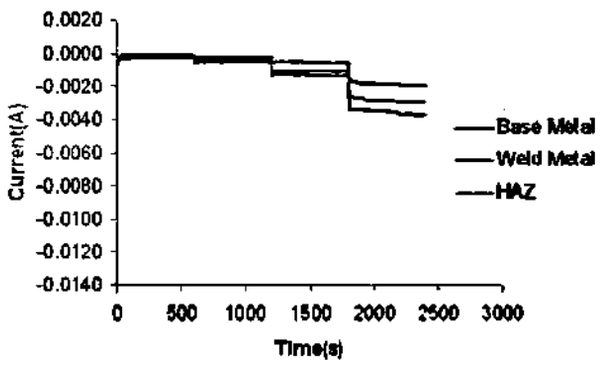

Fig. 6: Cathodic protection curve for Base Metal (at -500, -550, -600, 650) mV, Weld Metal (at -550, -650, -750, -850) mV and HAZ (at -650, -750, -850, -950) mV

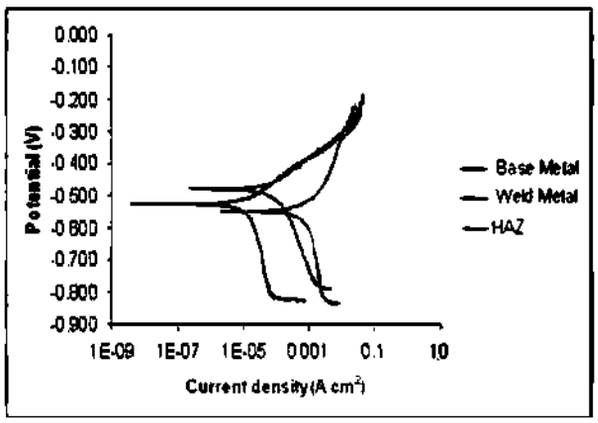

Fig. 5 : Polarisation curve for Base Metal,Weld Metal and HAZ

Table 4 : Electrochemical data derived from the polarisation curve

Specimen	Ecorr (V)	Corrosion Rate (mm/year)
Base Metal	-0.498	0.25
Weld Metal	-0.516	0.3
HAZ	-0.570	2.34

It is clearly observed from **Table 4** that corrosion rate is maximum in HAZ followed by weld metal and base metal in that order. Although the base metal and HAZ posses similar composition, higher corrosion rate in HAZ is likely due to alteration of microstructure and residual stress developed during welding. Again, the improvement of corrosion resistant in weld metal compared to HAZ is probably due to higher amount of copper. On the other hand, inferior corrosion resistant in weld metal compared to base metal is probably due to segregation effect which is encountered during welding.

3.4 Cathodic protection without stress

Based on the Ecorr values of base metal, weld metal and HAZ, four potentials for each zone of weldment were selected to study cathodic protection. The cathodic protection curves for base metal under (at -650, -725, -800, -875) mV, weld metal (at -800, -875, -950, -1025) mV and HAZ (at -875, -950, -1025, -1100) mV shown in **Fig. 6.**

In each zone of weldment, corrosion coefficient for each potential was evaluated and only minimum corrosion coefficient for base metal, HAZ and weld metal achieved for a given potential. The polarization potential, which attributed minimum corrosion coefficient, were considered as an adequate cathodic protection in corrosion fatigue test.

3.5 Corrosion Fatigue of Weld Metal

In the present investigation, fatigue test in air and environment was performed only in weld metal considering this part associated with more accident under corrosion. A comparison of fatigue crack growth behaviour of weld metal in air and 3.5% NaCl solution, both unprotected and at the cathodic potential based on minimum corrosion coefficient, for R=0.1 and cyclic frequency at 0.01Hz is shown in **Fig.7**. Corresponding cathodic protection curve (at -875 mV) of DMR (249A) Weld metal under fatigue loading is shown in **Fig. 8.**

The results as shown in **Fig.7** indicate that the crack growth resistance of weld metal is inferior in 3.5% NaCl solution to that of in air. The fatigue crack growth behavior of weld metal in 3.5% NaCl solution further show significant improvement of crack growth resistance under CP over free corrosion.

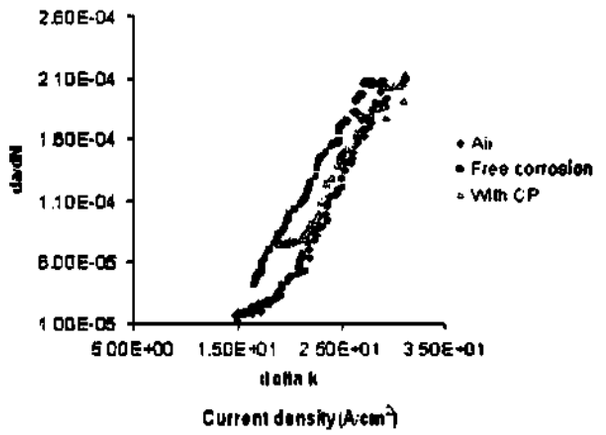

Fig.7: FCGR behavior of Weld Metal in Air, Free Corrosion Medium and with Cathodic Potential

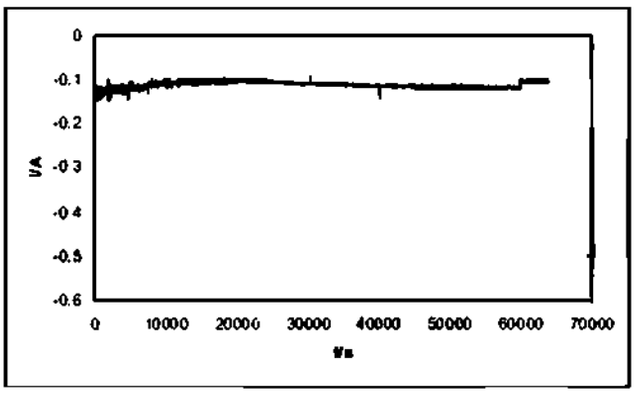

Fig. 8: Cathodic protection (at -875 mV) of DMR (249A) Weld metal under fatigue loading

The fatigue life enhancements from CP has been attributed by some authors to calcareous deposits (mainly $CaCO_3$ and Mg $(OH)_2$) within the nascent crack. This calcareous deposit was considered to form wedge at the crack tip, reducing the effective stress range, thus the early stages of crack growth are significantly delayed [12, 13]. However, similar behavior has been observed on plain tensile specimen tested in 3.5% NaCl where calcareous deposits do not occur [14]. It appears that the benefits of CP on fatigue crack growth rate, probably arising, from suppression of the metal dissolution process [14, 15].

In aqueous environments, anodic dissolution of metal at the crack tip and the entrance of hydrogen derived from the environment [16] into the crack-tip plastic zone occur simultaneously during corrosion fatigue crack propagation. Depending on mechanical (stress level, mode of loading, cyclic frequency, stress ratio, wave form), metallurgical (chemical composition, microstructure, grain boundary composition / orientation) and environmental (composition and concentration of solution, pH, potential, dissolved oxygen, temperature, flow rate) variables, one of the two mechanisms play a dominant role in crack propagation. It should also be noted that the intensity of anodic and or cathodic reactions in the vicinity of the crack tip, the hydrogen dependant properties of material and the hydrogen content in the crack tip zone also determine the controlling corrosion FCG mechanisms.

An increased generation of hydrogen under cathodic polarization enters into metal on the external surface of the specimen [16] and within the growing crack [17, 18]. FCG provides local breakdown of the passive film at the crack tip surface and produce a bare (film free) metal surface during the opening part of each stress cycle [19, 20 and 21]. The entry of the hydrogen promoted into the metal which transported under the driving force of the stress gradient to the region of higher dilation ahead of the crack leading to hydrogen embrittlement. The above arguments on susceptibility to HIC under cathodic polarization, however, fails to explain the decrease in corrosion FCG rate for applied cathodic potential of -875 mV in the present study. Recent observation on the effect of cathodic polarization indicated that crack growth rate accelerates when Kmax exceeded certain critical values corresponding to conditions when sufficient hydrogen has occurred at a certain characteristic distance [22, 23] ahead of the crack.

This will attain the critical combination of stress state and hydrogen concentration [24]. In line with the above findings, it is reasonable to believe that Kmax in the present study does not cross the critical value. Fujii and Smith [25] found that the fatigue crack growth rate acceleration occurred at a stress intensity range ΔK exceeded 30-40 $MPa\sqrt{m}$ at R=0.1 for the high strength HY – 130 steel in 0.6 M NaCl solution. The result obtained in this study conceive a possibility for similar mechanism in decelerating effect of cathodic polarization on crack growth rate up to ΔK of 32-35 and R = 0.1. Furthermore, the dominant mechanism in corrosion fatigue crack propagation was supported by fractographic observations. Transgranular fracture mode and some evidence of inelastic incremental crack advance occurring along the grain boundaries revealed in weld metal as shown in **Fig.9** also suggest that the critical combination of stress state and hydrogen concentrations has not been achieved ahead of the growing crack.

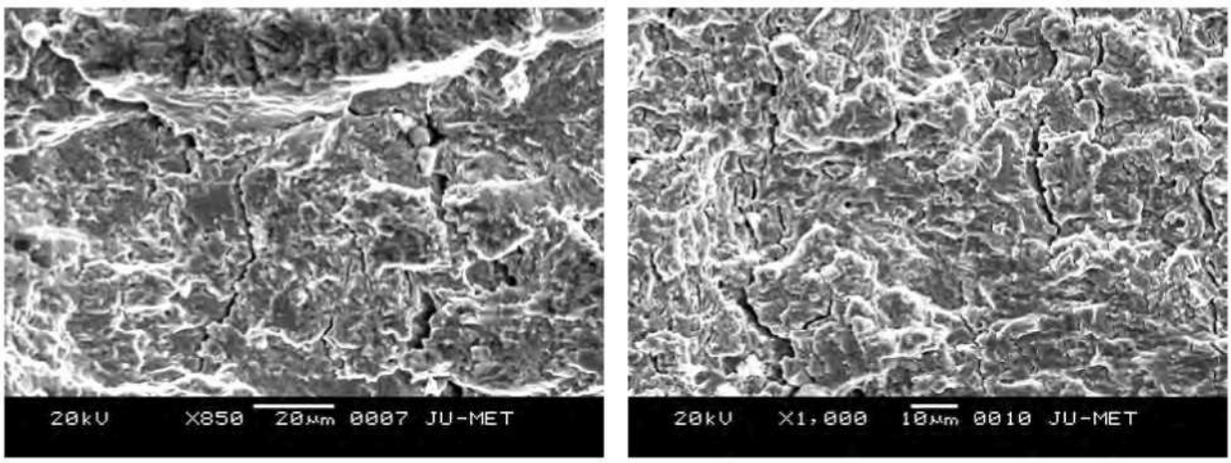

Fig. 9: Fatigue Fracture surfaces of Weld Metal

It has also been reported that sufficient or critical protection potential was closely related to the tensile strength of steels and the sensitivity to hydrogen embrittlement increased markedly with their strength [26, 27]. Previous work reported that the potential required to achieve full protection of carbon – manganese steels in aerated seawater is widely considered to be – 800 mV (Ag/AgCl) and this value is supported by DnV [28] and NACE [29]. However, recommended potentials range between – 750 and – 830 mV (Ag/AgCl) [30]. The present steel of DMR249A being higher strength than carbon – manganese steel, applied potential of -875mV could be considered as an appropriate in protecting the weld metal.

4.0 CONCLUSION

1. The crack growth resistance of weld metal is inferior in 3.5% NaCl solution to that of in air.
2. Optimum cathodic potential in unstressed condition was evaluated from the minimum corrosion coefficient among four potentials based on Ecorr value.
3. Preliminary results from the corrosion fatigue tests on weld metal in 3.5% NaCl solution at R=0.1 and cyclic frequency of 0.01 Hz suggest that optimum cathodic potential data (-875mV) determined in unstressed condition could be used to improve the corrosion fatigue life of weld metal in naval structure.

5.0 ACKNOWLEDGEMENT

The authors would like to thank Naval Research Board for financial support of the work and Mr. Suvasis Mukherjee for his help in corrosion fatigue test experiment.

6.0 REFERENCES:

1. Cyclic Fatigue of Steel Ship welded joints by Bureau Veritas: IIW/IIS DOC XIII 1169-85.
2. C. Batt and M. J. Robinson: British Corrosion Journal, 2002, Vol 37, No.1, pp. 31-36.
3. N. Rothwell and M. E. D. Turner : Mater. Performance, 1990, p.58
4. K. A. Lucas and M. J. Robinson: Corrosion Science, 1986, vol.26, no.9, pp 705-717.
5. C. Lindley and W. J. Rudd: Marine Structures, 2002, vol.14, pp. 397-416.
6. O. Grong and D. Matlock, "Micro structural development in mild and low alloy steel weldmetal", International Metal Review, 1986, Vol 31, No 1, pp. 27-48.
7. D. J. Abson and R. J. Pargeter, "Factors influencing the as – deposited strength, microstructure and toughness of manual metal arc welds suitable for C-Mn steel fabrication", International metals Review, 1986, Vol.31, No 4, pp-141-194.
8. J. Jang and J. E Indacochca, "Inclusion effects on submerged arc weld micro structure", Journal of Material Science , 1987, Vol 22, pp 687-700.
9. S. Liu, D. L. olon, S. Ibarra and O. Runnerstam, "oxygen as a welding parameter the role of light-metallography" ASW International 1993, vol.20, pp-31-44.
10. L. E Svensson and B. Gretoft, "Micro structural and Impact toughness of C-Mn weldmetal", welding journal, 1990, Vol 12, Dec , pp.454-461.

11. S. Liu and D. L. oho, " The role of inclusion in controlling HSLA steel weld microstructures", Welding Journal, 1986, Vol 66, June , pp. 139s – i49s.
12. O Vosikovsky , WR. Tyson Effects of cathodic protection on fatigue life of steel welded joints in seawater. Proceedings of the CANMET Workshop, Halifax, Nova Scotia, September 1986. pp. 1-43.
13. UKORSP 11, Summary Report.
14. H. Hu Fatigue and corrosion fatigue crack growth resistance of RQT 501 steel. PhD thesis, Department of Mechanical Engineering, University of Shefield, August 1997.
15. YZ Wang, RA Akid, KJ. Miller The effect of cathodic polarization on corrosion fatigue of a high strength steel in salt water. Fatigue Fract. Engg. Mater. Struct. 1995; pp.18(3):293,303.
16. T. G Owe Berg,. (1960) kinetics of absorption by metals of hydrogen from water and aqueous solutions, Corrosion 16, pp.198t-200t.
17. A. Turnbull, and M. Saenz de Santa Maria, predicting the kinetics of hydrogen generation at the tips of corrosion fatigue cracks in structural steel cathodically protected in sea water.corros.Sci.26,1988, pp. 601-628
18. T. Zakroczymski, Entry of hydrogen into iron alloys from the liquid phase. In: Hydrogen Degradation of Ferrous Alloys,(Edited by R. A.Oriani, J. P. Hirth and M. Smialowski), Noyes Publications, Park Ridge, 1985, pp.215-250
19. D. A. Jones, An unified mechanism of stress corrosion fatigue cracking. Metall.Trans.16A, 1985, pp.1133-1141.
20. H Masuda,. and S. Nishijima, Application of scratching electrode method for corrosion fatigue. Trans. Nat. Res. Inst Met.29, 1987, pp.44-50.
21. M Shimojo, Y Higo. and S Nunomura. Relation between the amount of fresh bare surface at the crack tip and the fatigue crack propagation rate. ISI. Int. 31, 1991, pp. 870-874.
22. P. Doig, and G. T. Jones, A model for the initiation of hydrogen embrittlement cracking at notches in gaseous hydrogen environments. Metall.Trans.8A, 1977,pp.1993-1998
23. K Akhurst,. A criterion for hydrogen induced fracture. In: Advances in Fracture Research–Fracture 81, Vol.4 (Edited by D. Francois, et.al.) Pergamon Press, oxford, (1982) pp.1899-1907.
24. A. R Troiano The role of hydrogen and other interstitials in the mechanical behavior of metals. Trans. ASM52, (1960), pp.54-80
25. C. T Fujii,. and J. A Smith,.) Environmental influences on the aqueous fatigue crack growth rates of HY-130 steel. In: corrosion Fatigue. Mechanics Metallurgy, Electro-chemistry and Engineering, ASTM STP 801.American society for Testing and Materials, Philadelphia, PA, 1983, pp.390-402.
26. H H Lee, H H Uhlig: "Corrosion fatigue of type 4140 high strength steel", Metal Trans., 1972; 3, p.2949 – 57.
27. Vasilenko II; Kapinos VI: the role of adsorption, dissolution and hydrogen embrittlement processes during the fatigue failure of steels in aggressive environment
28. Det Norske Veritas, Cathodic Protection Design, Veritas recommended practice RPB 401,March 1986.
29. National Association of Corrosion Engineers, control of corrosion of offshore steel pipelines, NACE publication RP-06-75 (Houstan, Texas), 1975.
30. J. N. Wanklyn, Input data for modeling Marine Cathodic protection ,cathodic protection theory and practice, Eds V. Ashworth & C. J. L. Booker, Publ Ellis Horwood, 1986, pp. 68-77.